Microchemical Journal 190 (2023) 108648

Contents lists available at ScienceDirect

Microchemical Journal

journal homepage: www.elsevier.com/locate/microc

Source determination of human and animal oral fluid stains on porous substrates by chemometrics-assisted ATR FTIR spectroscopy: A preliminary study

Cristina Cano-Trujillo [a,c,1], Anna Barbaro [a,b,c,1], Fernando E. Ortega-Ojeda [a,c,d], Carmen García-Ruiz [a,c], Gemma Montalvo [a,c,*]

[a] Universidad de Alcalá, Departamento de Química Analítica, Química Física e Ingeniería Química, Ctra. Madrid-Barcelona km 33,6, 28871 Alcalá de Henares, Madrid, Spain
[b] Studio Indagini Mediche E Forensi (SIMEF), via Nicolo da Reggio 4, 89128 Reggio Calabria, Italy
[c] Universidad de Alcalá, Instituto Universitario de Investigación en Ciencias Policiales, Libreros 27, 28801 Alcalá de Henares, Madrid, Spain
[d] Universidad de Alcalá, Departamento de Ciencias de la Computación, Ctra. Madrid-Barcelona km 33,6, 28871 Alcalá de Henares, Madrid, Spain

ARTICLE INFO

Keywords:
ATR FTIR
Oral fluid
Stains on substrates
Identification
Differentiation
Forensic science

ABSTRACT

Oral fluids are common evidence that can be found as stains on a variety of substrates at crime scenes. The porosity of the substrate may influence their collection and analysis. Moreover, companion animals, such as dogs, may appear in many scenarios or even be involved in a crime. Determining the source (identification and classification) of human and canine oral fluid stains on different substrates found at crime scene is important prior to DNA extraction to diminish laboratory cost and time efforts. In the present work, the potential of attenuated total reflection Fourier transform infrared spectroscopy (ATR FTIR) was explored to study how several types of porous substrates influence in the source determination of human and animal (canine) oral fluid stains. Results showed that the main bands of human or canine oral fluid stains were visible among the characteristic infrared bands of the porous substrates. This allowed the identification of human or animal (canine) oral fluid stains origin in the three types of papers and six fabrics porous substrates studied. Then, the application of Orthogonal Partial Least Square-Discriminant Analysis (OPLS-DA) models to the obtained infrared spectra, allowed the classification of human and canine oral fluid stains independently of the substrate they were deposited on. This approach could be developed for real forensic investigations to distinguish the source (identification and classification) of oral fluid stains as human or animal.

1. Introduction

Biological fluids are commonly found as stains on different types of substrates at a crime scene. Depending on the nature of the substrate, fluid detection changes. On porous substrates, the fluid penetrates the substrate, so the detected bands are weaker and may be overlapped by the bands of the substrate itself. On non-porous substrates, on the other hand, the fluids remain on the surface, so the spectra will be more intense and will not have any interference from the substrate [1]. In a crime scene, the presence of porous substrates as paper or fabrics is very common, being of forensic interest to explore analytical approaches able to determine the source (identification and classification) of biological fluid stains.

Oral fluid is a biological sample commonly found at crime scenes, as fluid or stains on different substrates, especially in cases involving sexual assaults and fights [2,3]. Companion animals, such as dogs, may appear in many crime scenes or even be involved in the crime. Oral fluid stains can be found in many samples, such as food, cutlery, glasses, cigarettes,

Abbreviations: ATR FTIR, attenuated total reflection Fourier transform infrared spectroscopy; GA, genetic algorithm; IR, infrared; LDA, linear discriminant analysis; OPLS-DA, orthogonal partial least square-discriminant analysis; OSC, orthogonal signal correction; PCA, principal component analysis; PLS, partial least squares; PLS-DA, partial least squares-discriminant analysis; SFA, significant factor analysis; SNV, standard normal variate.

* Corresponding author at: Universidad de Alcalá, Departamento de Química Analítica, Química Física e Ingeniería Química, Ctra. Madrid-Barcelona km 33,6, 28871 Alcalá de Henares, Madrid, Spain.
E-mail address: gemma.montalvo@uah.es (G. Montalvo).

[1] Both authors have contributed equally to this work.

https://doi.org/10.1016/j.microc.2023.108648
Received 13 March 2023; Accepted 14 March 2023
Available online 21 March 2023

spits, bites, etc. As DNA can be extracted from oral fluid, it is advantageous to know its source prior to perform DNA analysis to select only relevant samples that may be used as a probe, and to reduce laboratory costs and time efforts.

Saliva and oral fluid are not the same. Saliva is the secretion of parotic, sublingual, and submandibular glands (salivary glands) [4,5]. When saliva is mixed with other oral compounds, such as mucins or gingival fluid, is named oral fluid [5]. Oral fluid is composed mainly by water, electrolytes, mucus, enzymes, antibacterial components like antibodies, hormones, [2,4], and oral epithelial cells [3]. The canine oral fluid has high non-specific esterase, acid phosphatase, and pseudocholinesterase activity. It does not have amylase, while glycosylated proteins are common. In addition, canine oral fluid has a pH of 8.5, while the human oral fluid pH is 6.5–7.5; the buffering capacity and mineral concentrations are also higher in canine oral fluid than in human oral fluid [6].

To date, there are not confirmatory tests for oral fluid, only presumptive tests, which are destructive to the sample and not selective. Using alternate light source, oral fluid can be detected but it cannot be differentiated from other fluids. Amylase is a component of oral fluid used in the presumptive tests (*e.g.,* the starch-iodine test), but it is present in other bodily fluids too. There are even non-biological fluids that give false positives in the oral fluid presumptive tests, like in the Phadebas test reagent. Immunological and microscopy methods (that allow to confirm sample nature and origin) are commonly employed to identify oral fluid [2,7], but all of them are sample consuming.

Animal and human oral fluid are identical to the naked eye, but they are different at a biochemical level. These differences between the composition of the human and animal oral fluid may be used for their discrimination by vibrational spectroscopy. Attenuated total reflection Fourier transform infrared (ATR FTIR) spectroscopy is a vibrational spectroscopic technique with a high potential for the study of biological fluids. Vibrational spectroscopy is based on the measurement of the vibration of the molecules' bonds. As each molecular bond has its own vibrational characteristics [1,8], then each biological fluid have its own spectrum according to its composition. This become an advantage when the goal is to identify a sample or to differentiate it from other samples [2].

Raman and ATR FTIR spectroscopy are two types of vibrational spectroscopy. They are both complementary, as they detect different types of molecular vibrations. ATR FTIR spectroscopy basis lies in the changes of the dipole moment of the molecules after their excitation with electromagnetic radiation, while Raman spectroscopy depends on the polarizability of the molecules after their excitation with a laser radiation [8,9]. Using Raman spectroscopy, the spectroscopic signature of oral fluid was described by Virkler and Lednev [2]. They found that the spectra of oral fluid could be described by three components: one protein, which they suspect could be a mucin, one saccharide, like glycosaminoglycans from the mucus, and one amino acid, the arginine. They stated that the Raman spectral signature of oral fluid could be used to identify and differentiate oral fluid stains from other biological or non-biological fluids in a forensic context.

Although Raman spectroscopy is very selective and allows the identification of different biological fluids, it is strongly influenced by the characteristics of the substrate. ATR FTIR spectroscopy is more useful in this context because it has the advantage of not being much influenced by the substrates [10,11]. The disadvantage of an analysis by ATR FTIR is that it is strongly influenced by the presence of water, a highly polar molecule with an enormous signal in the infrared (IR) spectra. Nevertheless, the fluid stains are found dry at the crime scene, thus this is not a drawback for their analysis [12]. ATR FTIR spectroscopy is selective, fast, and non-destructive, which is imperative to maintain the integrity of the samples and avoid degradation, and it does not need chemical compounds that can be harmful for the analysts [10,12–15]. In this way, further analysis of the sample can be carried out with other analytical techniques [13–15].

Spectroscopic analysis of fluid stains results in a large amount of data that must be processed to obtain the most relevant information. The analysis and comparison of IR spectra of different biological fluid samples can be complex, as the differences are not always easily observed to the naked eye. Therefore, their interpretation by chemometric analysis of the data is usually used [16,17]. Chemometrics is defined as the application of mathematical and statistical analysis to chemistry [8,16].

Up to date, oral fluid stains have been analysed with ATR FTIR spectroscopy by different authors. Sharma *et al.* analysed oral fluid stains to create chemometric models that allowed the discrimination of different types of bodily fluids from semen [10]. Quinn and Elkins analysed oral fluid stains in five different substrates (cotton, woven nylon, glass, wood, and paper) to compare its ATR FTIR spectra with those from peripheral and menstrual blood, semen, and breastmilk, but they did not use chemometrics [20]. Oral fluid stains, along blood, semen, urine, and sweat, were analysed by Takamura *et al.* using ATR FTIR spectroscopy to build a chemometric model that could differentiate all of them. They combined partial least square (PLS), linear discriminant analysis (LDA), Q-statistics, and a dichotomous classification tree in a model that allowed to correctly discriminate the five bodily fluids (fresh and aged) and to exclude non-biological fluids [17]. Elkins used ATR FTIR to study the spectra of 12 different biological samples, including oral fluid samples. She also analysed non-biological fluid substances. The samples were placed on cotton. Oral fluid and blood were also analysed on paper. She made a deep study of the different characteristic bands of each biological and non-biological sample, but chemometrics were not used for the discrimination [21].

Other authors tried to differentiate between human and animal bodily fluids (blood and semen), but none of them did focus on human and animal oral fluid. Virkler and Lednev used Raman spectroscopy to differentiate between human, canine, and feline blood [22]. Using a portable Raman spectrometer, Fujihara *et al.* analysed human, cow, horse, sheep, pig, rabbit, chicken, rat, mouse, cat, and dog blood [23]. Mistek-Morabito and Lednev analysed human and animal blood (cat, dog, rabbit, horse, cow, pig, opossum, raccoon, deer, elk, and ferret) with ATR FTIR spectroscopy [24]. Kumar *et al.* also used ATR FTIR spectroscopy, but they employed human, pig, and goat blood to make the stains [25]. Elkins analysed sheep blood to compare with human blood using ATR FTIR spectroscopy [21]. Li *et al.* and Wang *et al.* had a different objective, to study bloodstain aging. For that purpose, they used equine blood [26,27]. Li *et al.* analysed the bloodstains with hyperspectral imaging [26], while Wang *et al.* employed laser-induced breakdown spectroscopy (LIBS) [27]. Hyperspectral imaging was also used by Silva *et al.*, but with a different bodily fluid, as they wanted to differentiate human and animal semen [28].

To our knowledge, there are not studies that focus on the source (identification and classification) determination of human and animal (canine) oral fluid stains on porous substrates. Thus, the main goal of this research was to explore the potential of ATR FTIR spectroscopy assisted with chemometrics for the study of the source of oral fluid stains in porous substrates in order to: (i) find the IR spectral characteristics of human and animal (canine) oral fluid stains on two types of porous substrates (paper and fabrics) for the identification of the origin (human or animal) of the stains and (ii) explore chemometric approaches to discriminate human and animal oral fluid stains on those substrates.

2. Materials and methods

2.1. Samples preparation

Human and animal (canine) oral fluid were employed. The human oral fluid sample was obtained from one donor (a 40-year-old woman) by spitting directly into a tube. For the animal oral fluid, the sample was obtained from one donor (a 5-years old female dog of the West Highland white terrier breed) by directly withdrawing the oral fluid from the mouth with a pipette. The animal had not eaten or drunk anything for at

least half an hour before the extraction.

Nine different substrates were used to prepare the oral fluid stains: kitchen, general tissue, and white office paper, white towel, corduroy, yellow cotton, pink cotton, denim, and polyester fabrics. The substrates were cut into 5x5 cm pieces and measured before making the stains to obtain their pure spectra. 10 μL of oral fluid (human or canine) were deposited on the surface of the substrates. The samples were analysed after 24 h of their deposition on the different porous substrates. They were left to dry at ambient conditions (25 °C), not exposed to direct sunlight, and kept in a low flow cabinet. One human and one animal oral fluid stain were also made on a glass slide to measure the spectra of the oral fluid stains in a non-porous and inert substrate with a low contribution to the IR spectra.

The samples were taken according to the protocol approved by the Universidad de Alcalá (UAH) Ethics and Research Committee (ref. n°CEIP/HU/2021/1/002 and CEIP/2022/3/045).

2.2. Instrumentation

The oral fluid stains were measured with a Nicolet iS10 FT-IR Spectrometer (Thermo Fisher Scientific, Waltham, Massachusetts, United States) and the Smart iTR ATR with diamond crystal component equipped with the OMNIC v9.6 software (Thermo Fisher Scientific, Waltham, Massachusetts, United States). The resolution was 4 cm^{-1}, with 128 scans in the absorbance mode. The spectral range measured was comprised from 650 cm^{-1} to 4000 cm^{-1}.

In order to verify the signal reproducibility, each sample was measured seven times, moving it every two measurements. This movement was random leading to random measurement points.

2.3. Data analysis

The OMNIC gathered-data from the spectrometer was imported into The Unscrambler X v10.4 (CAMO-Aspen Technology, Houston, United States). This software was used to pre-process the data before making the models. To do so, standard normal variate (SNV) normalisation followed by a baseline offset correction, and Savitzky-Golay smoothing (2nd order polynomial and 7 smoothing points) was applied.

The matrices were then imported into Microsoft Excel v2008 (Microsoft Corporation, Redmond, Washington, United States). After the pre-processing, orthogonal partial least square-discriminant analysis (OPLS-DA) models were created using SIMCA v17.02 (Sartorius, Göttingen, Germany). In this work, OPLS-DA models were used for the identification of the origin (human or canine) of the oral fluid stains. The OPLS-DA model was selected because of its great capacity to discriminate the samples according to the variable of interest. It come from the union between PLS, which is a regression method, and orthogonal signal correction (OSC), a pre-processing method, with the aim of discriminating the data. OPLS-DA is composed of three matrices that are divided into matrix Y, matrix X correlated with Y, and matrix X uncorrelated with Y, also called orthogonal [18]. The parameter R^2X determines how well the model fits the data, which can have a value between 1 (perfect fit) or 0 (no fit). Another relevant parameter is Q^2, which indicates the predictive ability of the model. Similarly, its value varies between 1 (perfect predictive ability) and 0 (no predictive ability) [19].

The graphics were created using OriginPro 2021v (OriginLab Corporation, Northampton, Massachusetts, United States). All the spectra shown in the figures is the result of the average of seven measurements made for each one of the oral fluid stains. To admit a region as a band of interest, the signal-to-noise ratio had to be at least 3.

3. Results and discussion

First, oral fluid stains were characterised in a neutral substrate for the spectral characterization of the human and animal (canine) oral fluid stains. Glass slides were selected because they were a non-porous and inert substrate for ATR FTIR spectroscopy where no bands of its own were detected among the deposited stains' bands. This allowed to characterise the studied oral fluid stains as there was no influence of the substrate. Fig. 1 shows the human and canine oral fluid spectra of stains on glass slides.

In the human oral fluid stain spectrum, the 650–1080 cm^{-1} region was assigned to some bands from carbohydrates and sugars [20], including α-amylase [17]. The four amides bands were also assigned: Amide III at 1240 cm^{-1}, Amide II at 1540 cm^{-1}, Amide I at 1633 cm^{-1}, and Amide A at 3279 cm^{-1} [17]. This last band overlap with the O-H stretch region band at 3261 cm^{-1} [20]. The band at 2053 cm^{-1} was attributed to the presence of thiocyanate anions (SCN^-) [17,20]. The bands at 2852 and 2920–2960 cm^{-1} were assigned to the symmetric and asymmetric C-H stretching of the lipids' ester groups [17]. The band at 1400 cm^{-1} was attributed to the methyl bending of the amino acid chains [20].

Although the canine oral fluid IR spectrum has not been published elsewhere, a comparison can be made with the human oral fluid spectrum in order to determine which bands may result significant. As seen in Fig. 1, the 650–1080 cm^{-1} region from the carbohydrates and sugars [20] is similar in both spectra. The band at 1233 cm^{-1} can be assigned to the Amide III, whilst the small bands at 1541 cm^{-1} and 1644 cm^{-1}, can be attributed to the Amide II and Amide I, respectively [17,20]. The band from the amino acid chains methyl bending that appeared at around 1400 cm^{-1} in the human spectrum, may correspond to the bands in the 1387–1456 cm^{-1} region of the canine spectrum. The lipids can be assigned to the 2870–2981 cm^{-1} region, while the Amide A can be at the 3200–3300 cm^{-1} region [17] along the O-H stretch groups [20]. This is an indicative assignment since it is not based on a previously published assignment on canine oral fluid analysed with infrared spectroscopy.

The spectra of human and canine oral fluids with their standard deviations can be seen in Figure S1. The signal differences in each wavelength are not significant when comparing different measurements of each sample, hence the results are reliable.

At the crime scene, the oral fluid stains can be found in different type of substrates, such as cans, cigarettes, papers, clothes, flooring, etc. Hence, it is of utmost importance to be able to identify oral fluid stains in different substrates. Depending on the nature of the substrates on which the biological fluids are deposited, the spectrum obtained after ATR FTIR spectroscopic analysis may vary. In case of porous substrates, the characteristic bands of the fluid may be masked by the substrate's own bands. This happens because the fluid penetrates the inner layers of the substrate. To study this phenomenon, we selected three types of paper

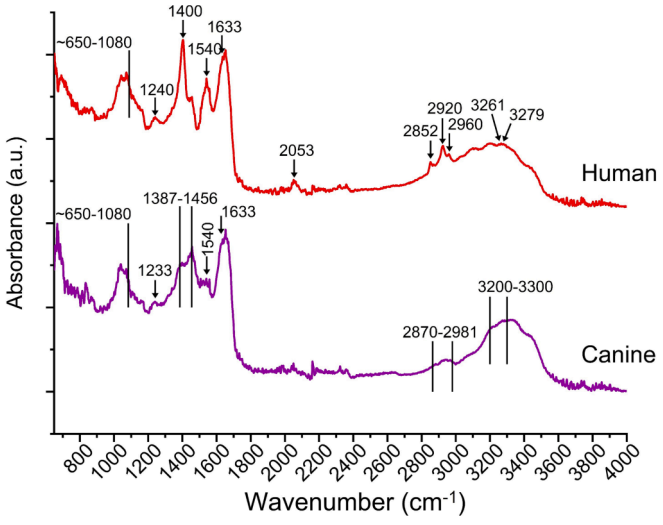

Fig. 1. IR spectra of human and animal (canine) oral fluid stains on glass slides as neutral substrate.

and six fabrics of different colours as porous substrates.

The first three substrates are filter, tissue, and white office paper, based on cellulose, kaolinite, and calcium carbonate composition. The characteristic bands and their assignment are shown in Table 1. As expected, most of the bands coincide in all three spectra, for instance, the 3300 cm^{-1} from the OH-O, the 2950–2800 cm^{-1} bands from CH stretching, or the 1160 cm^{-1} band from C-OH stretching in cellulose. However, there are some other bands that do not appear in the filter and tissue paper: the 1430–1420 cm^{-1} region from the cellulose, and the 1420–1410 cm^{-1} region and the 710 cm^{-1} band from the calcium carbonate [29,30].

As all papers have a cellulose-based composition, only office paper is shown in Fig. 2 because of the spectral similitudes among these substrates. The ~650–1200 cm^{-1} region is practically identical in all three spectra, except for small decreases in the intensity of the 710 and 873 cm^{-1} bands, which correspond to calcium carbonate, in the human and animal (canine) oral fluid spectra regarding the office paper spectra. An intensity decrease is also observed in the 1428 cm^{-1} band of cellulose [29,30]. Four bands increase their intensity in the oral fluid spectra: 1240 cm^{-1} (Amide III/phospholipids [17,20]), 1380 cm^{-1} (methyl bending of amino acid chains [20]), 1530 cm^{-1} (Amide II), and 1640 cm^{-1} (Amide I) [17,20]. Thus, Fig. 2 shows the office paper's spectrum together with the spectra of human and animal (canine) oral fluid stains on office paper as substrate.

The other six fabric substrates have cotton as their main component, so they share most of the bands and their spectra were also very similar among them. Cotton fibres are mostly composed of cellulose (97–98 %). Other elements such as pectins, proteins, waxes, fattys, and mineral salts make up the remaining components 2–3 % [31–33]. The six fabrics are listed in Table 2. The first four fabrics are white, yellow, pink, and black cotton. They have the same characteristic bands, except for the 1000 cm^{-1} band (C-O stretch), which only appeared on the pink and black cotton [31,32]. The main difference among them is the colour of the substrate, which was not a handicap in the IR spectral signals for the identification of the oral fluid stains according to the substrate.

Corduroy is slightly different, as it has 5 bands that are not present in the previous fabrics. Those are the bands at 2918 cm^{-1} (asymmetric CH_2 stretch), 2850 cm^{-1} (symmetric CH_2 stretch), 1730 cm^{-1} (C = O stretching), 1650 cm^{-1} (O-H bending), and 1539 cm^{-1} (aromatic ring C = C stretching) [31,32].

Table 1
Characteristic bands and their functional groups' assignment of filter, tissue, and office paper. The (*) marks the bands that only appear in the office paper spectrum according to references [29,30].

Characteristic bands	Bonds assignment
~3300	OH—O
2950–2800	CH stretching in CH, CH_2, CH_3, symmetric
2890	C—O—C
1636	O—H
1500–1200	COH in plane bending; CCH and OCH deformation stretching; HCH bending and wagging
1428	
1430–1420*	
1420–1410*	
1380–1300	CH and C—OH deformation vibrations
1314	C—CH_2
1200–900	C—C and C—O stretching, asymmetric in phase ring stretching, antisymmetric bridge COC stretching, as well as CCH and OCH deformation vibrations
1160	C—OH
1120–1000	C—O and C—O—C stretching vibrations
1026	C—H
1005	
<900	CCC, CCO, COC, OCO and COH deformation and torsional vibrations
873	
710*	

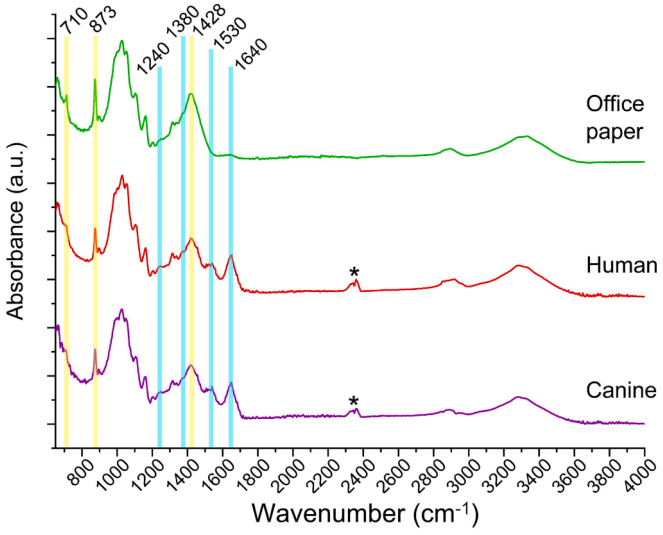

Fig. 2. IR spectra of human and animal (canine) oral fluid stains on office paper along with the pure spectra of the substrate. The bands that change their intensity are marked. The bands from the human and animal (canine) oral fluid spectra that increase their intensity with respect to the pure office paper spectrum are colored in blue, while the yellow lines indicate a reduction of the oral fluid bands' intensity. The * mark the bands from CO_2 between 2300 and 2400 cm^{-1}.

Among the different cotton fabrics studied, denim was chosen to show oral fluid stains on fabrics, as it is one of the most commonly found at crime scene. Fig. 3 shows the spectra of denim and human and animal (canine) oral fluid stains on denim. Five bands are highlighted because their intensity increase in the oral fluid spectra compared to the denim's spectrum. The bands at 1530 cm^{-1} and 1640 cm^{-1} were assigned to the Amide II and Amide I, respectively [17,20]. The 2854 and 2943 cm^{-1} bands were attributed to the asymmetric and symmetric C-H stretching from lipids [17], while the 2908 cm^{-1} was assigned to a methyl stretch [20].

The porosity of the studied substrates and the characteristics of the human and canine oral fluid, which is mainly composed by water, allowed the fluid to penetrate in the inner layers of the papers and fabrics. Because of this, the spectra obtained after the analysis of the oral fluid stains on those substrates is dominated by the substrates' bands. The only oral fluid's bands visible in those spectra allowing their identification are the Amide II and Amide I bands at 1530 and 1640 cm^{-1}. A similar result was obtained by Zapata *et al.* after the analysis of semen, urine, and vaginal fluid on cotton with external reflection FTIR [34].

Quinn and Elkins also stated that the bands of venous and menstrual blood, semen, oral fluid, and breastmilk as stains on porous substrates (woven nylon, cotton, paper, and wood) could be identified, but their intensity was lower compared to the fluids analysed directly on the ATR FTIR [20]. Results of Sharma *et al.* also agree with those presented in this work. They analysed menstrual blood on cotton, denim, polyester, paper, and sanitary napkins with ATR FTIR. The significant bands of menstrual blood could be detected, especially the Amide I and Amide II bands (1645 and 1533 cm^{-1}, respectively), but the intensity was lower and the substrates dominated the spectra [12].

The observable differences between the spectra of the paper and cotton substrates and the spectra of both human and canine oral fluid stains on these substrates do not allow objective clear identification of the fluid. To solve this, OPLS-DA models were explored to differentiate the substrates without stains from the substrates with oral fluid stains.

First, two OPLS-DA models were created. The first OPLS-DA model for the three paper substrates (Fig. 4A) had an R^2X of 97 % and a Q^2 of 87 %. According to these results, the human and canine oral fluid stains show the same behaviour in the three different papers. Looking again at

Table 2
Characteristic bands and their functional groups' assignment of fabrics according to references [31,32]. The ([a]) mark the band that only appear in the pink cotton. The ([b]) mark the band that only appear in the black cotton.

Substrate	Characteristic bands	Assignment
Cotton (white, yellow, pink, black)	3333	O—H stretching
	2899	CH_2 asymmetric stretch
	2853	CH_2 symmetric stretch
	1644	O—H bending
	1429	C—H wagging (in-plane bending)
	1368	CH bending (deformation stretch)
	1335	OH in-plane bending
	1315	CH wagging
	1279	CH deformation stretch
	1246	OH in-plane bending
	1203	OH in-plane bending
	1161	Asymmetric bridge C—O—C
	1108	Asymmetric bridge C—O—C
	1055	Asymmetric in-plane ring stretch
	1030	C—O stretch
	998[a,b]	C—O stretch
	899	Asymmetric out-of-phase ring stretch: C_1-O-C_4; β glucosidic bond
	700–650	O—H out-of-plane bending
Corduroy	3333	O—H stretching
	2918	Asymmetric CH_2 stretch
	2850	Symmetric CH_2 stretch
	1730	C═O stretching
	1650	O—H bending
	1539	Aromatic ring C═C stretching
	1428	C—H wagging (in-plane bending)
	1367	C—H bending (deformation stretch)
	1335	OH in-plane bending
	1314	CH wagging
	1278	CH deformation stretch
	1247	OH in-plane bending
	1203	OH in-plane bending
	1159	Asymmetric bridge C—O—C
	1107	Asymmetric bridge C—O—C
	1053	Asymmetric in-plane ring stretch
	1030	C—O stretch
	1000	C—O stretch
	700–650	O—H out-of-plane bending
Denim	~3600–3100	O—H stretching N—H stretching
	2901	C—H stretching
	1630	O—H bending
	1315	C—H wagging
	1161	C—O—C stretching
	1030	C—O stretching

Fig. 2, although it was difficult to differentiate the spectrum of office paper without the stains from the human and animal oral fluid stains' spectra on office paper, and these two from each other, using this OPLS-DA model, a complete discrimination was achieved.

Fig. 4B shows the second OPLS-DA model for the six fabrics as substrates. It had an $R^2X = 97$ % and a $Q^2 = 87$ %. This model, like the previous one, also makes it possible to discriminate the fabric substrates without stains from oral fluid stains on these fabrics, and also both human and animal (canine) oral fluids. The colour of the tissues did not seem to play a role in discriminating oral fluid stains, as they all behaved in the same way. Again, this result was in line with that obtained by Zapata *et al.*, [34] who was able to discriminate semen, urine, and vaginal fluid when they were analysed as stains on coloured cotton using external reflection ATR FTIR and a principal component analysis (PCA).

The results of these two models indicate that, despite the strong influence that porous substrates have on the ATR FTIR analysis, the technique is sensitive enough to detect differences between the unstained substrates, the substrates stained with human oral fluid and the same substrates with canine oral fluid stains.

To distinguish human from animal (canine) oral fluid stains, the potential of OPLS-DA models was also explored. Fig. 5 shows the

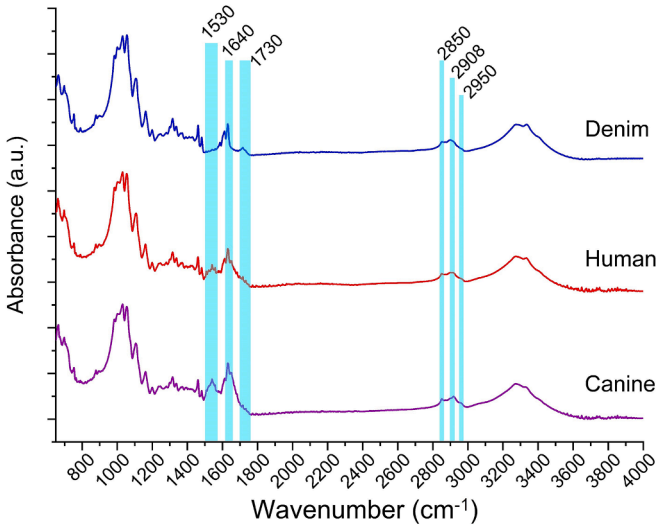

Fig. 3. IR spectra of human and animal (canine) oral fluid stains on denim along with the spectrum of the substrate. The bands from the human and animal (canine) oral fluid stain spectra that increase their intensity with respect to the denim spectrum are colored in blue.

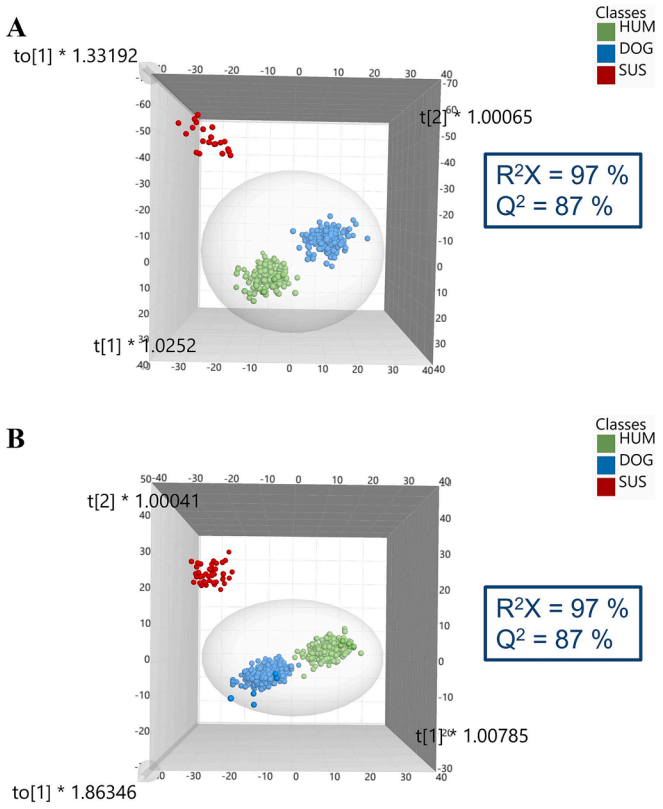

Fig. 4. 3D scatters plot of the two OPLS-DA models. A) OPLS-DA model which discriminates the three paper substrates from the human and animal oral fluid stains on them, and one from each other. B) OPLS-DA model which discriminates the six fabric substrates from the human and animal oral fluid stains on them, and one from each other. HUM: human oral fluid stains (green dots). DOG: canine oral fluid stains (blue dots). SUS: substrate (red dots).

complete discrimination of the oral fluid stains from human (green dots) and animal (blue dots) oral fluid stains on the nine different substrates used in this work. Despite the data dispersion, the human green-coloured samples are well separated from the animal blue-coloured

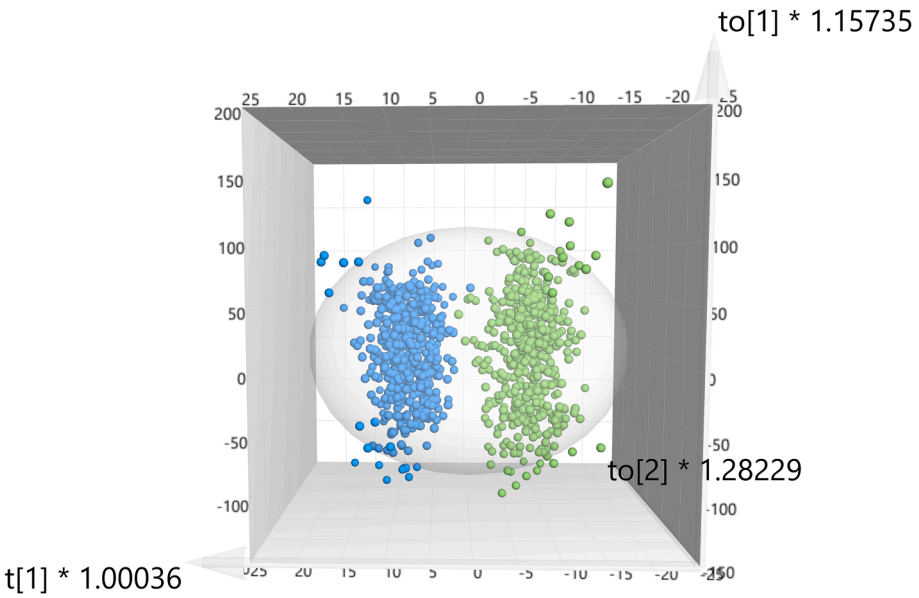

Fig. 5. 3D scatters plot of the OPLS-DA model in which the IR spectra are discriminated according to the oral fluid origin (human or canine) independently of the substrate where they are deposited on. HUM: human oral fluid stains (green dots). DOG: canine oral fluid stains (blue dots).

samples. The model explains 97 % of the variance in X (R^2X) and it has a prediction capacity of 83 % (Q^2).

The OPLS-DA models enabled to differentiate samples according to species at the individual substrate's level, and also when the stains in all studied substrates were analysed as a whole. In other words, the substrate is not a problem for the discrimination of the oral fluid stains' source (human or canine). This result is very promising because it could be applied *in situ* at the crime scene using portable ATR FTIR systems.

These are also novel results with oral fluid stains analysed by ATR FTIR since Virkler and Lednev were the first authors that discriminated human, canine, and feline blood but using Raman spectroscopy with chemometrics. They combined significant factor analysis (SFA) with PCA and achieved the complete discrimination of the three species [22]. Fujihara *et al.* analysed human, cow, horse, sheep, pig, rabbit, chicken, cat, dog, rat, and mouse blood on gauze with a portable Raman spectrometer. The human and animal blood stains were discriminated using a PCA [23]. Mistek-Morabito and Lednev used ATR FTIR and a combination of a genetic algorithm (GA) and a partial least squares-discriminant analysis (PLS-DA) to discriminate human from animal blood. Eleven animal species were analysed: dog, cat, rabbit, horse, cow, pig, opossum, racoon, deer, elk, and ferret. None of them was classified as human by the chemometric model [24].

This is a preliminary study involving only one donor (human and canine) because the main aim was to evaluate the effect of common porous substrates on the analysis of oral fluid stains. The study needs to be expanded using a larger number of donors, both human and canine, to obtain greater variability and to make chemometric models more robust. In addition, it is relevant to consider the donor diet, habits, diseases, etc. because they can lead to variation in the composition or characteristics of the biological fluids [1–3,35].

4. Conclusions and future perspectives

At the crime scene, bodily fluid stains can appear in many substrates and under different conditions. The porous or non-porous nature of a substrate determines the ability to carry out the stains' analysis because the substrate signal may hinder the stains' signals. ATR FTIR spectroscopy analysis led to the relevant fact that main bands of human or animal oral fluid stains were visible among the characteristic IR spectral bands of the porous substrates.

Using ATR FTIR spectroscopy combined with chemometric analysis (OPLS-DA), this work proves that oral fluid stains can be identified on different porous substrates (three papers and six fabrics). Two OPLS-DA models have clearly discriminated the human and canine oral fluid stains on the two types of porous substrates.

A third OPLS-DA model proved a clear discrimination of the human and canine oral fluid stains by their source independently of the substrate they were deposited on.

From a scientific point of view, this work is novel, and it adds knowledge to IR spectroscopy. It has also forensic relevance, as its application could positively aid criminal investigations. This promising preliminary study requires to be expanded by increasing the number and variety of sample donors (humans and animals) in order to obtain a more robust predictive model applicable to determine the source (identification and classification) of an unknown oral fluid stain independently of the substrates where it is deposited on. Rising the number of donors, more variability will be accounted for, making the OPLS-DA models more robust.

The availability of portable devices would allow to apply ATR FTIR spectroscopic analysis *in situ* at the crime scene. Before these systems can be used, it is necessary to carry out a study with them, as the conditions vary from those of the bench-top devices currently used at laboratories.

Declaration of Competing Interest

The authors declare that they have no known competing financial interests or personal relationships that could have appeared to influence the work reported in this paper.

Data availability

Data will be made available on request.

Acknowledgements

This study is part of the Real-tIme on-site forensic tracE qualificatioN project (RISEN, SU-FCT02-2018-2019-2020-883116), which is funded by the European Union's Horizon 2020 research and innovation program. Authors thank the funding from this program under the grant agreement No 883116. C. Cano-Trujillo thanks the University of Alcalá, Spain for her pre-doctoral grant (grant No. 572765/EXP 2022/00185). The authors also thanks Johana Saldaña (funding PEJ-2020-TL/IND-

18159) for her help and support with the sample preparation and analysis.

Appendix A. Supplementary data

Supplementary data to this article can be found online at https://doi.org/10.1016/j.microc.2023.108648.

References

[1] A. Takamura, K. Watanabe, T. Akutsu, H. Ikegaya, T. Ozawa, Spectral mining for discriminating blood origins in the presence of substrate interference via attenuated total reflection fourier transform infrared spectroscopy: postmortem or antemortem blood? Anal. Chem. 89 (2017) https://doi.org/10.1021/acs.analchem.7b01756.

[2] K. Virkler, I.K. Lednev, Forensic body fluid identification: the Raman spectroscopic signature of saliva, Analyst. 135 (2010) 512–517, https://doi.org/10.1039/b919393f.

[3] E. Al-Hetlani, L. Halámková, M.O. Amin, I.K. Lednev, Differentiating smokers and nonsmokers based on Raman spectroscopy of oral fluid and advanced statistics for forensic applications, J. Biophotonics. 13 (2020) e201960123.

[4] A. Zhang, H. Sun, X. Wang, Saliva Metabolomics opens door to biomarker discovery, disease diagnosis, and treatment, Appl. Biochem. Biotech. 168 (2012) 1718–1727, https://doi.org/10.1007/s12010-012-9891-5.

[5] V. D'Elia, G. Montalvo García, C. García Ruiz, Spectroscopic trends for the determination of illicit drugs in oral fluid, Appl. Spectrosc. Reviews 50 (9) (2015) 775–796, https://doi.org/10.1080/05704928.2015.1075206.

[6] S. Pasha, T. Inui, I. Chapple, S. Harris, L. Holcombe, M.M. Grant, The saliva proteome of dogs: variations within and between breeds and between species, Proteomics. 18 (2018) 1700293-n/a 10.1002/pmic.201700293.

[7] K. Virkler, I.K. Lednev, Analysis of body fluids for forensic purposes: from laboratory testing to non-destructive rapid confirmatory identification at a crime scene, Forensic Sci. Int. 188 (2009) 1–17, https://doi.org/10.1016/j.forsciint.2009.02.013.

[8] A.R. Weber, I.K. Lednev, Crime clock – Analytical studies for approximating time since deposition of bloodstains, Forensic Chem. 19 (2020), 100248, https://doi.org/10.1016/j.forc.2020.100248.

[9] F. Zapata, A. López-Fernández, F. Ortega-Ojeda, G. Montalvo, C. García-Ruiz, A practical beginner's guide to Raman microscopy, Appl. Spectrosc. Rev. 56 (6) (2021) 439–462, https://doi.org/10.1080/05704928.2020.1797761.

[10] S. Sharma, R. Singh, Detection and discrimination of seminal fluid using attenuated total reflectance Fourier transform infrared (ATR FT-IR) spectroscopy combined with chemometrics, J. Leg. Med. 134 (2020) 411–432, https://doi.org/10.1007/s00414-019-02222-x.

[11] I. Gregório, F. Zapata, C. García-Ruiz, Analysis of human bodily fluids on superabsorbent pads by ATR-FTIR, Talanta 162 (2017) 634–640, https://doi.org/10.1016/j.talanta.2016.10.061.

[12] S. Sharma, R. Chophi, R. Singh, Forensic discrimination of menstrual blood and peripheral blood using attenuated total reflectance (ATR)-Fourier transform infrared (FT-IR) spectroscopy and chemometrics, J. Leg. Med. 134 (2020) 63–77, https://doi.org/10.1007/s00414-019-02134-w.

[13] S. Sharma, R. Singh, Detection of vaginal fluid stains on common substrates via ATR FT-IR spectroscopy, J. Leg. Med. 134 (2020) 1591–1602, https://doi.org/10.1007/s00414-020-02333-w.

[14] F. Zapata, A. López-Fernández, F.E. Ortega-Ojeda, G. Quintanilla, C. García-Ruiz, G. Montalvo, Introducing ATR-FTIR spectroscopy through analysis of acetaminophen drugs: practical lessons for interdisciplinary and progressive learning for undergraduate students, J. Chem. Educ. 98 (2021) 2675–2686, https://doi.org/10.1021/acs.jchemed.0c01231.

[15] S. Sharma, R. Chophi, J.K. Jossan, R. Singh, Detection of bloodstains using attenuated total reflectance-Fourier transform infrared spectroscopy supported with PCA and PCA–LDA, Med. Sci. Law. 61 (2021) 292–301, https://doi.org/10.1177/00258024211010926.

[16] C.K. Muro, K.C. Doty, L. de Souza Fernandes, I.K. Lednev, Forensic body fluid identification and differentiation by Raman spectroscopy, Forensic Chem. 1 (2016) 31–38, https://doi.org/10.1016/j.forc.2016.06.003.

[17] A. Takamura, K. Watanabe, T. Akutsu, T. Ozawa, Soft and robust identification of body fluid using fourier transform infrared spectroscopy and chemometric strategies for forensic analysis, Sci. Rep. 8 (2018) 8459, https://doi.org/10.1038/s41598-018-26873-9.

[18] M. Bylesjö, M. Rantalainen, O. Cloarec, J.K. Nicholson, E. Holmes, J. Trygg, OPLS discriminant analysis: combining the strengths of PLS-DA and SIMCA classification, J. Chemometrics. 20 (2006) 341–351, https://doi.org/10.1002/cem.1006.

[19] L. Ortiz Herrero, Development of new methodologies for dating in the forensic field, combining analytical techniques with multivariate regression treatments (2021) 318.

[20] A.A. Quinn, K.M. Elkins, The differentiation of menstrual from venous blood and other body fluids on various substrates using ATR FT-IR spectroscopy, J. Forensic Sci. 62 (2017) 197–204, https://doi.org/10.1111/1556-4029.13250.

[21] K.M. Elkins, Rapid presumptive fingerprinting of body fluids and materials by ATR FT-IR spectroscopy, J. Forensic Sci. 56 (2011) 1580–1587, https://doi.org/10.1111/j.1556-4029.2011.01870.x.

[22] K. Virkler, I.K. Lednev, Blood species identification for forensic purposes using raman spectroscopy combined with advanced statistical analysis, Anal. Chem. 81 (2009) 7773–7777, https://doi.org/10.1021/ac901350a.

[23] J. Fujihara, Y. Fujita, T. Yamamoto, N. Nishimoto, K. Kimura-Kataoka, S. Kurata, Y. Takinami, T. Yasuda, H. Takeshita, Blood identification and discrimination between human and nonhuman blood using portable Raman spectroscopy, J. Leg. Med. 131 (2017) 319–322, https://doi.org/10.1007/s00414-016-1396-2.

[24] E. Mistek-Morabito, I.K. Lednev, Discrimination between human and animal blood by attenuated total reflection Fourier transform-infrared spectroscopy, Commun. Chem. 3 (2020) 1–6, https://doi.org/10.1038/s42004-020-00424-8.

[25] R. Kumar, K. Sharma, V. Sharma, Bloodstain age estimation through infrared spectroscopy and Chemometric models, Sci. Justice. 60 (2020) 538–546, https://doi.org/10.1016/j.scijus.2020.07.004.

[26] B. Li, P. Beveridge, W.T. O'Hare, M. Islam, The age estimation of blood stains up to 30 days old using visible wavelength hyperspectral image analysis and linear discriminant analysis, Sci. Justice. 53 (2013) 270–277, https://doi.org/10.1016/j.scijus.2013.04.004.

[27] Q. Wang, G. Teng, Y. Zhao, X. Cui, K. Wei, Identification and determination of the bloodstains dry time in the crime scenes using laser-induced breakdown spectroscopy, IEEE Photonics J. 11 (2019) 1–12, https://doi.org/10.1109/JPHOT.2019.2912580.

[28] C.S. Silva, M.F. Pimentel, J.M. Amigo, R.S. Honorato, C. Pasquini, Detecting semen stains on fabrics using near infrared hyperspectral images and multivariate models, TrAC, Trends Anal. Chem. 95 (2017) 23–35, https://doi.org/10.1016/j.trac.2017.07.026.

[29] C.S. Silva, M.F. Pimentel, J.M. Amigo, C. García-Ruiz, F. Ortega-Ojeda, Chemometric approaches for document dating: handling paper variability, Anal. Chim. Acta. 1031 (2018) 28–37, https://doi.org/10.1016/j.aca.2018.06.031.

[30] J. Zięba-Palus, A. Wesełucha-Birczyńska, B. Trzcińska, R. Kowalski, P. Moskal, Analysis of degraded papers by infrared and Raman spectroscopy for forensic purposes, J. Mol. Struct. 1140 (2017) 154–162, https://doi.org/10.1016/j.molstruc.2016.12.012.

[31] C. Chung, M. Lee, E.K. Choe, Characterization of cotton fabric scouring by FT-IR ATR spectroscopy, Carbohydr. Polym. 58 (2004) 417–420, https://doi.org/10.1016/j.carbpol.2004.08.005.

[32] P. Peets, I. Leito, J. Pelt, S. Vahur, Identification and classification of textile fibres using ATR-FT-IR spectroscopy with chemometric methods, Spectrochim. Acta, Part A 173 (2017) 175–181, https://doi.org/10.1016/j.saa.2016.09.007.

[33] T.L. Silva, A.L. Cazetta, P.S.C. Souza, T. Zhang, T. Asefa, V.C. Almeida, Mesoporous activated carbon fibers synthesized from denim fabric waste: efficient adsorbents for removal of textile dye from aqueous solutions, J. Cleaner Prod. 171 (2018) 482–490, https://doi.org/10.1016/j.jclepro.2017.10.034.

[34] F. Zapata, M. Fernández-de-la-Ossa, C. García-Ruiz, Differentiation of body fluid stains on fabrics using external reflection fourier transform infrared spectroscopy (FT-IR) and chemometrics, Appl. Spectrosc. 70 (2016) 654–665, https://doi.org/10.1177/0003702816631303.

[35] C. Cano-Trujillo, C. García-Ruiz , F.E. Ortega-Ojeda , F. Romolo , G. Montalvo, Forensic analysis of biological fluid stains on substrates by spectroscopic approaches and chemometrics: A review , (Sent to Forensic Science International).